Journal of Organometallic Chemistry, *462* (1993) 353–363

JOM 23647

Studies on the complex $[Rh\{\sigma,\eta^5\text{-}7,9\text{-}C_2B_9H_{10}[C(H)C_6H_4Me\text{-}4]\text{-}10\}(CO)(PPh_3)]$; crystal structure of the compound $[Rh(CO)(PPh_3)\{\eta^5\text{-}7,9\text{-}C_2B_9H_{10}[C(H)(C_6H_4Me\text{-}4)(PEt_3)]\text{-}10\}]$ *

Justin E. Goldberg and John C. Jeffery

School of Chemistry, The University, Bristol BS8 1TS (UK)

F. Gordon A. Stone

Department of Chemistry, Baylor University, Waco, TX 76798-7348 (USA)

(Received February 10, 1993)

Abstract

Treatment of CO-saturated CH_2Cl_2 solutions of $[NEt_4][Rh(CO)(PPh_3)(\eta^5\text{-}7,9\text{-}C_2B_9H_{11})]$ with $[Mn(\equiv CC_6H_4Me\text{-}4)(CO)_2(\eta^5\text{-}C_5H_4Me)][BCl_4]$ affords the complex $[Rh\{\sigma,\eta^5\text{-}7,9\text{-}C_2B_9H_{10}[C(H)C_6H_4Me\text{-}4]\text{-}10\}(CO)(PPh_3)]$. The latter reacts with $K[BH(CHMeEt)_3]$ in the presence of $[NEt_4]Cl$ to yield $[NEt_4][Rh(CO)(PPh_3)\{\eta^5\text{-}7,9\text{-}C_2B_9H_{10}(CH_2C_6H_4Me\text{-}4)\text{-}10\}]$, and with tertiary phosphines ($L = PMe_3$, PEt_3, or PMe_2Ph) to give the zwitterionic complexes $[Rh(CO)(PPh_3)\{\eta^5\text{-}7,9\text{-}C_2B_9H_{10}\text{-}[C(H)(C_6H_4Me\text{-}4)(L)]\text{-}10\}]$. The crystal structure of the product with $L = PEt_3$ has been determined, thereby firmly establishing the structure of this class of complex. The reaction between $[AuCl(PPh_3)]$ and the species with $L = PMe_3$ in the presence of $TlBF_4$ affords the dimetal compound $[RhAu(CO)(PPh_3)_2\{\eta^5\text{-}7,9\text{-}C_2B_9H_{10}[C(H)(C_6H_4Me\text{-}4)(PMe_3)]\text{-}10\}][BF_4]$. The NMR spectra of the new compounds are reported, and discussed in relation to their structures.

1. Introduction

The salts $[X][Rh(CO)(L)(\eta^5\text{-}7,n\text{-}C_2B_9H_9R'_2)]$ (**I**, $X = NEt_4$, or $N(PPh_3)_2$; $n = 8$, $L = CO$ or PPh_3, $R' = H$ or Me; $X = NEt_4$, $n = 9$, $L = PPh_3$, $R' = H$) [1**] react with a variety of metal complexes to yield products in which a carborane rhodium fragment is σ bonded to another metal atom (Mn, Re, Co, Rh, Ir, Pt, Cu, or Au) with its attendant ligands [2]. However, reactions between the reagents $[X][Rh(CO)(L)(\eta^5\text{-}7,8\text{-}C_2B_9H_9\text{-}R'_2)]$ (**Ia–d**) and the manganese compounds $[Mn(\equiv CR)\text{-}(CO)_2(\eta^5\text{-}C_5H_4Me)][BCl_4]$ ($R = C_6H_4Me\text{-}4$ or $C_6H_3Me_2\text{-}2,6$) followed an unexpected course, affording the mononuclear rhodium complexes $[Rh\{\sigma,\eta^5\text{-}7,8\text{-}C_2B_9H_8[C(H)R]\text{-}10\text{-}R'_2\text{-}7,8\}(CO)(L)]$ ($R = C_6H_4Me\text{-}4$, $R' = H$, $L = PPh_3$ (**IIa**); or CO (**IIb**); $R = C_6H_3Me_2\text{-}2,6$, $R' = H$, $L = PPh_3$ (**IIc**); $R = C_6H_4Me\text{-}4$, $R' = Me$, $L = PPh_3$ (**IId**); or CO (**IIe**)) [2e, 3], instead of the expected dimetal species in which an alkylidyne group bridges a Mn–Rh bond. The formation of the compounds **IIa–e** probably proceeds via intermediates with metal–metal bonds which facilitate transfer of the alkylidyne group from manganese to rhodium, a process which is evidently followed by insertion of the alkylidyne into the B(10)–H bond. The manganese fragment is released as $[Mn(CO)_3(\eta^5\text{-}C_5H_4Me)]$, as discussed elsewhere [2e,3].

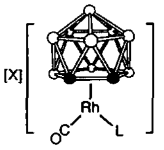

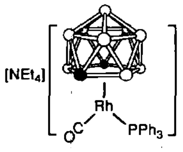

○ BH

	X	L	●
Ia	NEt_4	CO	CH
Ib	$N(PPh_3)_2$	PPh_3	CH
Ic	NEt_4	CO	CMe
Id	NEt_4	PPh_3	CMe

Ie ●CH

Correspondence to: Professor F.G.A. Stone.

* This paper is dedicated to Professor M.F. Lappert on the occasion of his 65th birthday, and in gratitude for his long-standing friendship.

** Reference with asterisk indicates a note in the list of references.

0022-328X/93/$6.00

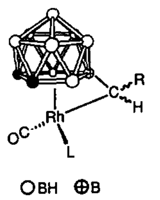

	R	L	●
IIa	C_6H_4Me-4	PPh_3	CH
IIb	C_6H_4Me-4	CO	CH
IIc	$C_6H_3Me_2$-2,6	PPh_3	CH
IId	C_6H_4Me-4	PPh_3	CMe
IIe	C_6H_4Me-4	CO	CMe

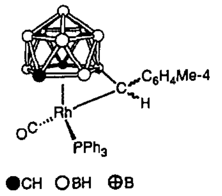

IIf

In this paper we report the reaction between $[NEt_4][Rh(CO)(PPh_3)(\eta^5\text{-}7,9\text{-}C_2B_9H_{11})]$ (**Ie**) and $[Mn(\equiv CC_6H_4Me\text{-}4)(CO)_2(\eta^5\text{-}C_5H_4Me)][BCl_4]$, as well as some reactions of the product $[Rh\{\sigma,\eta^5\text{-}7,9\text{-}C_2B_9H_{10}[C(H)C_6H_4Me\text{-}4]\text{-}10\}(CO)(PPh_3)]$ (**IIf**). The latter complex is a polytopal isomer of **IIa**, having a 2,1,7-RhC_2B_9 icosahedral core structure, as opposed to the 3,1,2-RhC_2B_9 cage frameworks in the species **IIa–e**.

2. Results and discussion

Treatment of CO-saturated CH_2Cl_2 solutions of **Ie** with $[Mn(\equiv CC_6H_4Me\text{-}4)(CO)_2(\eta^5\text{-}C_5H_4Me)][BCl_4]$ gave, after column chromatography on alumina, orange crystals of $[Rh\{\sigma,\eta^5\text{-}7,9\text{-}C_2B_9H_{10}[C(H)C_6H_4Me\text{-}4]\text{-}10\}(CO)(PPh_3)]$ (**IIf**). As observed previously [2e, 3], the $Mn(CO)_2(\eta^5\text{-}C_5H_4Me)$ fragment is eliminated as $[Mn(CO)_3(\eta^5\text{-}C_5H_4Me)]$. Hence the reaction is carried out in the presence of CO to increase the yield of **IIf**.

Compound **IIf** was characterised by the data given in Tables 1–3. The spectroscopic properties are similar to those of **IIa** and are entirely consistent with the structure shown. Thus the presence of the *B*C(H)-C_6H_4Me-4 group is revealed in the $^{11}B\text{-}\{^1H\}$ NMR spectrum (Table 3), in which a diagnostic resonance corresponding in intensity to one boron atom is seen at δ 8.8, a value almost identical with that (δ 8.7) found in the spectrum of $[NEt_4][Mo\{\sigma,\eta^5\text{-}7,8\text{-}C_2B_9H_8[C(H)C_6H_4Me\text{-}4]\text{-}10\text{-}Me_2\text{-}7,8\}(CO)_3]$, the anion of which also has a $C(H)C_6H_4Me$-4 moiety bridging the metal atom and the cage [4]. Interestingly, the $^{11}B\text{-}\{^1H\}$ NMR resonance for the *B*$C(H)C_6H_4Me$-4 group in **IIa** at δ 17.4 [3], is appreciably more deshielded than in **IIf**.

TABLE 1. Analytical [a] and physical data for the rhodium complexes

Compound	Colour	Yield (%)	$\nu_{max}(CO)$ [b] cm^{-1}	Analysis (%)	
				C	H
IIf $[Rh\{\sigma,\eta^5\text{-}7,9\text{-}C_2B_9H_{10}[C(H)C_6H_4Me\text{-}4]\text{-}10\}(CO)(PPh_3)]$	orange	83	2022vs	55.9 (55.4)	5.4 (5.3)
IIId $[NEt_4][Rh(CO)(PPh_3)\{\eta^5\text{-}7,9\text{-}C_2B_9H_{10}(CH_2C_6H_4Me\text{-}4)\text{-}10\}]$ [c]	dark green	97	1923vs	57.6 (58.5)	7.4 (7.2)
IIIe $[NEt_4][Rh(CO)(PPh_3)\{\eta^5\text{-}7,9\text{-}C_2B_9H_{10}[C(H)(Me)(C_6H_4Me\text{-}4)]\text{-}10\}]$ [c,d]	red	98 (39)	1921s	59.0 (59.0)	7.3 (7.3)
IVa $[Rh(CO)(PPh_3)\{\eta^5\text{-}7,9\text{-}C_2B_9H_{10}[C(H)(C_6H_4Me\text{-}4)(PMe_3)]\text{-}10\}]$	green-yellow	92	1927vs	54.5 (54.5)	6.0 (6.0)
IVb $[Rh(CO)(PPh_3)\{\eta^5\text{-}7,9\text{-}C_2B_9H_{10}[C(H)(C_6H_4Me\text{-}4)(PEt_3)]\text{-}10\}]$	yellow	84	1923vs	55.6 (56.3)	6.5 (6.5)
IVc $[Rh(CO)(PPh_3)\{\eta^5\text{-}7,9\text{-}C_2B_9H_{10}[C(H)(C_6H_4Me\text{-}4)(PMe_2Ph)]\text{-}10\}]$	yellow	78	1924vs	57.1 (58.0)	6.0 (5.8)
V $[NEt_4][Rh(COMe)\{\sigma,\eta^5\text{-}7,9\text{-}C_2B_9H_{10}[C(H)C_6H_4Me\text{-}4]\text{-}10\}(PPh_3)]$ [c,e]	red	98 (59)	1600m br	59.0 (59.0)	7.3 (7.3)
VI $[RhAu(CO)(PPh_3)_2\{\eta^5\text{-}7,9\text{-}C_2B_9H_{10}[C(H)(C_6H_4Me\text{-}4)(PMe_3)]\text{-}10\}][BF_4]$	pale green	98	1972vs	47.9 (48.0)	4.7 (4.6)

[a] Calculated values are given in parentheses.
[b] Measured in CH_2Cl_2. All spectra show a broad band at *ca.* 2550 cm^{-1} due to B–H absorptions.
[c] Compound also contains nitrogen. For: **IIId** 1.9 (1.8%); **IIIe** and **V** 1.8 (1.8%).
[d] Compound formed as an inseparable 2:3 mixture with **V**. Yield quoted is overall value for mixture; figure in parentheses calculated yield for **IIIe**. Microanalytical data is for the isomer mixture. See text.
[e] Compound formed as a 3:2 mixture with **IIIe**, see footnote d.

TABLE 2. (footnotes)

[a] Chemical shifts δ in ppm, coupling constants in Hz, measurements at ambient temperatures in CD_2Cl_2, R = C_6H_4Me-4.
[b] Signals due to BH groups appear as broad unresolved resonances in the range δ *ca.* −2 to +3.
[c] Hydrogen-1 decoupled, chemical shifts are positive to high frequency of $SiMe_4$ (δ 0.0).
[d] Spectrum measured in $CDCl_3$.
[e] Compound formed as an inseparable 2:3 mixture with **V**; peaks assigned on basis of integration of ^1H and $^{31}P\text{-}\{^1H\}$ NMR spectra and intensities and shifts of the resonances in the $^{13}C\text{-}\{^1H\}$ NMR spectrum. See text.
[f] Measured in $CDCl_3$ on a sample with $[N(PPh_3)_2]^+$ as the counter-ion.
[g] Peaks marked with an asterisk due to minor isomer.
[h] Formed as an inseparable 3:2 mixture with **IIIe**. See footnote e.

TABLE 2. ^{1}H and ^{13}C NMR data [a] for the complexes

Compound	^{1}H [b] (δ)	^{13}C [c] (δ)
IIf	0.71 [s, 1H, CH($C_2B_9H_{10}$)], 2.17 (s, 3H, Me-4), 2.88 [s, 1H, CH($C_2B_9H_{10}$)], 6.37 [br s, 1H, BC(*H*)R], 6.80 –7.90 (m, 19H, Ph and C_6H_4)	[d] 191.1 [d of d, CO, *J*(RhC) 73, *J*(PC) 22], 141.9 [C^1(C_6H_4)], 137.3 [C^4(C_6H_4)], 133.6–128.5 (Ph and C_6H_4), 80.4 [br, B*C*(H)R], 54.1, 53.0 ($C_2B_9H_{10}$), 21.5 (Me-4)
IIId	1.03 [s, 1H, CH($C_2B_9H_{10}$)], 1.23 [t of t, 12H, NCH$_2$*Me*, *J*(HH) 7, *J*(NH) 2], 2.17 [s, 1H, CH($C_2B_9H_{10}$)], 2.30 (s, 3H, Me-4), 2.45, 2.54 [(AB), 2H, BCH$_2$, *J*(AB) 12], 3.15 [q, 8H, NC*H*$_2$Me, *J*(HH) 7], 6.90, 7.10 [(AB)$_2$, 4H, C_6H_4, *J*(AB) 8], 7.27–7.39 (m, 15H, Ph)	198.3 [d of d, CO, *J*(RhC) 93, *J*(PC) 21], 145.0 [C^1(C_6H_4)], 137.5 [d, C^1(Ph), *J*(PC) 38], 134.1 [d, C^2(Ph), *J*(PC) 12], 132.1 [C^4(C_6H_4)], 129.4 [C^2(C_6H_4)], 129.2 [d, C^4(Ph), *J*(PC) 2], 128.2 [C^3(C_6H_4)], 127.9 [d, C^3(Ph), *J*(PC) 9], 53.0 [t, N*C*H$_2$Me, *J*(NC) 3], 45.6, 41.7 ($C_2B_9H_{10}$), 33.7 (vbr, B*C*H$_2$R), 21.1 (Me-4), 7.8 (NCH$_2$*Me*)
IIIe [e]	0.43 [s, 1H, CH($C_2B_9H_{10}$)], 1.23 [t of t, 12H, NCH$_2$*Me*, *J*(HH) 7, *J*(NH) 2], [f] 1.25 [d, 3H, BCH*Me*, *J*(HH) 7][f], 2.00 (s, 3H, Me-4), 2.21 [s, 1H, CH($C_2B_9H_{10}$)], [f] 3.06 [q, br, 1H, BC*H*Me, *J*(HH) 7], 3.11 [q, 8H, NC*H*$_2$Me, *J*(HH) 7], 6.92, 7.10 [(AB)$_2$, 4H, C_6H_4, *J*(AB) 8], 7.20–7.38 (m, 15H, Ph)	198.2 [d of d, CO, *J*(RhC) 92, *J*(PC) 21], 150.8 [C^1(C_6H_4)], 137.4 [d, C^1(Ph), *J*(PC) 37], 134.3 [d, C^2(Ph), *J*(PC) 12], 132.1 [C^4(C_6H_4)], 129.2 [C^2 or C^3(C_6H_4)], 129.1 [d, C^4(Ph), *J*(PC) 2], 128.3 [C^2 or C^3(C_6H_4)], 128.0 [d, C^3(Ph), *J*(PC) 10], 52.9 (N*C*H$_2$Me), 46.2, 41.8 ($C_2B_9H_{10}$), 33.7 [vbr, B*C*(H)(Me)R], 23.4, 21.0 (Me), 7.7 (NCH$_2$*Me*)
IVa [g]	0.76 [s, 1H, CH($C_2B_9H_{10}$)], 1.67, * 1.72 [d, 9H, PMe, *J*(PH) 13], 2.42 [d, 3H, Me-4, *J*(PH) 2], 2.51, * 2.76 [s, 1H, CH($C_2B_9H_{10}$)], 4.06 [d, 1H, BC(*H*)R, *J*(PH) 18], 7.04–7.63 (m, 19H, Ph and C_6H_4)	196.9 [d of d of d, CO, *J*(RhC) 92, *J*(PC) 21 and 4], 136.9 [d, C^1(C_6H_4), *J*(PC) 4], 136.5 [d, C^1(Ph), *J*(PC) 40], 134.4 [d, C^2(C_6H_4), *J*(PC) 7], 134.0 [d, C^2(Ph), *J*(PC) 12], 132.7 [d, br, C^2(C_6H_4), *J*(PC) 7], 130.3, 130.0 [br, C^3(C_6H_4)], 129.6 [d, C^4(Ph), *J*(PC) 2], 128.1 [d, C^3(Ph), *J*(PC) 10], 127.2 [br, C^4(C_6H_4)], 45.3 (vbr, $C_2B_9H_{10}$), 44.7 ($C_2B_9H_{10}$), 33.7 [vbr, B*C*(H)R], 21.2, * 19.7 (Me-4), 11.3, * 10.6 [d, PMe, *J*(PC) 54]
IVb [g]	0.75 [s, 1H, CH($C_2B_9H_{10}$)], 1.10 [d of d of d, 9H, PCH$_2$*Me*, *J*(PH) 17, *J*(HH) 8 and 8], * 1.71 (m, 3H, PC*H*$_2$Me), 1.97 [d of d of q, 3H, PCH_AH_BMe, *J*(H_AH_B) 20, *J*(H_{Me}H) 8, *J*(PH) 8], * 2.14 (m, 3H, PC*H*$_2$Me), 2.24 [d of d of q, 3H, PCH_AH_BMe, *J*(H_AH_B) 20, *J*(H_{Me}H) 8, *J*(PH) 8], 2.49, * 2.59 [s, 1H, CH($C_2B_9H_{10}$)], 4.32 [d, br, 1H, BC(*H*)R, *J*(PH) 21], 6.99–7.58 (m, 19H, Ph and C_6H_4)	197.0 [d of d of d, CO, *J*(RhC) 92, *J*(PC) 22 and 4], 136.8 [d, C^1[C_6H_4), *J*(PC) 3], 136.5 [d, C^1(Ph), *J*(PC) 40], 134.1 [d, C^2(C_6H_4), *J*(PC) 8], 134.0 [d, C^2(Ph), *J*(PC) 12], 133.0 [d, C^2(C_6H_4), *J*(PC) 8], 130.2 [C^4(C_6H_4)], 129.7 [d, C^3(C_6H_4), *J*(PC) 2], 129.5 [d, C^4(Ph), *J*(PC) 2], 128.5 [d, C^3(C_6H_4), *J*(PC) 5], 128.1 [d, C^3(Ph), *J*(PC) 10], 45.6 (vbr, $C_2B_9H_{10}$), 44.7 ($C_2B_9H_{10}$), 33.9 [vbr, B*C*(H)R], 21.2, * 19.7 (Me-4), 13.8, * 12.2 [d, P*C*H$_2$Me, *J*(PC) 47], * 8.5, 6.6 [d, PCH$_2$*Me*, *J*(PC) 5]
IVc [g]	* 0.71, 0.78 [s, 1H, CH($C_2B_9H_{10}$)], 1.85, * 2.13 [d, 3 H, PMe, *J*(PH) 13], * 2.16 [d, 3H, Me-4, *J*(PH) 3], 2.24, * 2.26 [d, 3H, PMe, *J*(PH) 13], 2.35 [d, 3H, Me-4, *J*(PH) 3], 2.45 [s, 1H, CH($C_2B_9H_{10}$)], * 3.80, 4.52 [d, br, 1H, BC(*H*)R, *J*(PH) 21], 6.91–7.71 (m, 24H, Ph and C_6H_4)	197.1 [d of m, CO, *J*(RhC) 95], 136.7–123.7 (Ph and C_6H_4), 45.9, 44.7 ($C_2B_9H_{10}$), 38.5 [vbr, B*C*(H)R], 21.2 (Me-4), 10.1, 9.9 [d x 2, PMe, *J*(PC) 54]
V [h]	0.90 [s, 1H, CH($C_2B_9H_{10}$)], 1.23 [t of t, 12H, NCH$_2$*Me*, *J*(HH) 7, *J*(NH) 2], 1.86 [s, 1H, CH($C_2B_9H_{10}$)], 2.10, 2.29 (s x 2, 6H, COMe and Me-4), 3.11 [q, 8H, NC*H*$_2$Me, *J*(HH) 7], 4.35 [d, br, 1H, BC(*H*)R, *J*(PH) 3], 6.61, 6.84 [(AB)$_2$, 4H, C_6H_4, *J*(AB) 8], 7.20–7.38 (m, 15H, Ph)	243.3 [d of d, *C*(O)Me, *J*(RhC) 32, *J*(PC) 13], 150.3 [d of d, C^1(C_6H_4), *J*(RhC) 4, *J*(PC) 4], 136.6 [d, C^1(Ph), *J*(PC) 35], 134.0 [d, C^2(Ph), *J*(PC) 13], 131.4 [C^4(C_6H_4)], 128.9 [C^4(Ph)], 128.1 [C^2 or C^3(C_6H_4)], 127.7 [d, C^3(Ph), *J*(PC) 9], 126.9 [C^2 or C^3(C_6H_4)], 57.6 [vbr, B*C*(H)R], 52.9 (N*C*H$_2$Me), 41.3 [d, C(O)*Me*, *J*(PC) 3], 39.4, 34.5 ($C_2B_9H_{10}$), 21.2 (Me-4), 7.7 (NCH$_2$*Me*)
VI	1.07 [s, 1H, CH($C_2B_9H_{10}$)], 1.75 [d, 9H, PMe, *J*(PH) 13], 2.53 (s, 3H, Me-4), 3.44 [s, 1H, CH($C_2B_9H_{10}$)], 3.67 [d, 1H, BC(H)R, *J*(PH) 22], 7.13–7.57 (m, 34H, Ph and C_6H_4)	194.1 [d of m, CO, *J*(RhC) 76], 138.3 [d, C^1(C_6H_4), *J*(PC) 4], 134.6–127.7 (Ph and C_6H_4), 57.9, 51.4 ($C_2B_9H_{10}$), 37.2 [vbr, B*C*(H)R], 21.3 (Me-4), 10.6 [d, PMe, *J*(PC) 54]

This difference must be associated with the different core structures in the two compounds, *viz.*, 2,1,7-RhC_2B_9 *versus* 3,1,2-RhC_2B_9. That the peak in the ^{11}B-{^1H} NMR spectrum of **IIf** at δ 8.8 is due to the boron nucleus of the *B*C(H)C_6H_4Me-4 fragment was confirmed by the observation that the signal remained a singlet in a fully coupled ^{11}B spectrum, whereas all the other resonances in the range δ 0.5 to -17.9 became doublets [*J*(HB) *ca.* 140 Hz] in accord with these signals being due to cage BH groups.

The formula of **IIf** is depicted with the C(H)C_6H_4Me-4 group attached to B(10) rather than to the unique B(8) atom which separates the two carbons in the open pentagonal face of the cage ligating the rhodium. Although there is no firm NMR evidence for this assignment, the substantial difference in chemical shifts (δ 0.71 and 2.88) in the ^1H NMR spectrum (Table 2) of the two inequivalent cage CH vertices does suggest the less symmetrical arrangement with one CH vertex adjacent to the BC(H)C_6H_4Me-4 group and the other separated from it by a BH group. That this structural assignment for **IIf** is correct is strongly supported by the results of the X-ray diffraction study of a derivative, described below.

The ^1H and ^{13}C-{^1H} NMR spectrum of **IIf** also confirmed the presence of the BC(H)C_6H_4Me-4 group with a broad singlet at δ 6.37 in the former spectrum for the BC(*H*) proton, and a broad resonance in the latter spectrum at δ 80.4 for the B*C*(H) carbon nucleus. The broadness of both peaks is attributed to unresolved ^{11}B–^{1}H and ^{11}B–^{13}C coupling, respectively. In the ^{13}C-{^1H} NMR spectrum the resonance for the CO ligand occurs as the anticipated doublet of doublets at δ 191.1 [*J*(RhC) 73, *J*(PC) 22 Hz], and the signals for the two inequivalent cage CH vertices are seen (measured in $CDCl_3$ rather than CD_2Cl_2) at δ 54.1 and 53.0.

The ^{31}P-{^1H} NMR spectrum of **IIf** shows a single broad doublet [δ 32.0, *J*(RhP) 145 Hz] at room temperature. This same pattern persists in the spectrum measured at -70°C, indicating the presence of only one species in solution and the absence of fluxionality. This is in marked contrast with compounds **IIa** and **IId** which show a duplication of NMR peaks in accord with an equilibrium between two diastereoisomers. This behaviour is attributed to the chiral C(H)R fragments being able to adopt two orientations relative to the Rh(CO)(PPh_3) moiety, with the PPh_3 and R groups

TABLE 3. ^{11}B and ^{31}P NMR data [a] for the complexes

Compound	^{11}B [b] (δ)	^{31}P [c] (δ)
IIf	8.8 (s, 1B, BCHR), 0.5 (1B), -10.4 (2B), -13.8 (2B), -17.9 (3B)	32.0 [d, br, PRh, *J*(RhP) 145]
IIId	-0.1 (s, 1B, BCHR), -11.9 (1B), -12.9 (1B), -14.9 (2B), -21.1 (1B), -25.2 (2B), -28.8 (1B)	35.7 [d, PRh, *J*(RhP) 164]
IIIe [d]	3.0 [s, 1B, BC(H)(Me)R], -11.6 to -28.4 (vbr, 8B)	36.1 [d, PRh, *J*(RhP) 166]
IVa [e]	* -4.1, -5.2 (s, 1B, BCHR), -13.1 (1B), -14.5 (2B), -16.8 (1B), -22.9 (1B), -23.7 (1B), -25.9 (1B), -26.8 (1B)	36.5 [d, br, PRh, *J*(RhP) 168], * 26.6, 25.6 (s, PMe_3)
IVb [e]	-5.0, * -6.8 (s, 1B, BCHR), -13.1 (1B), -14.4 (2B), -16.9 (1B), -22.8 (1B), -23.7 (1B), -25.8 (1B), -26.6 (1B)	38.5, * 38.4 (s, PEt_3), 36.4 [d, vbr, PRh, *J*(RhP) 164]
IVc [e]	* -3.7, -5.1 (s, 1B, BCHR), -13.1 (1B), -14.6 (2B), -16.8 (1B), -22.9 (1B), -23.7 (1B), -25.9 (1B), -26.8 (1B)	36.3 [d, br, PRh, *J*(RhP) 164], * 25.9, 24.4 (s, PMe_2Ph)
V [f]	3.0 (s, 1B, BCHR), -11.6 to -28.4 (vbr, 8B)	30.2 [d, PRh, *J*(RhP) 198]
VI	0.4 (s, 1B, BCHR), -1.2 (1B, BF_4), -2.8 to -24.1 (vbr, 8B)	34.1 [d, br, PRh, *J*(RhP) 126], 33.7 (s, PMe_3), 30.7 [d, PAu, *J*(RhP) 4]

[a] Chemical shifts (δ) in ppm, coupling constants in Hz, measurements in CD_2Cl_2 at ambient temperatures.

[b] Hydrogen-1 decoupled, chemical shifts are positive to high frequency of $BF_3 \cdot Et_2O$ (external). R = C_6H_4Me-4.

[c] Hydrogen-1 decoupled, chemical shifts are positive to high frequency of 85% H_3PO_4 (external).

[d] Formed as a mixture with V; peak assignments based on rel. int. (see text).

[e] Peaks marked with asterisk are due to minor isomer.

[f] Formed as a mixture with IIIe. See footnote d and text.

having either a *cisoid* or *transoid* relationship with each other. However, in the crystalline state the latter arrangement occurs in **IIa** [3], and we assume that this *transoid* structure exists for **IIf** also. As a consequence of the dynamic behaviour of **IIa**, the $^{31}P\text{-}\{^1H\}$ NMR spectrum at −50°C shows two resonances at δ 35.1 [d, *J*(RhP) 147 Hz] and 34.0 [d, *J*(RhP) 143 Hz] with relative intensity 3:2. These signals almost coalesce in the room temperature spectrum. The dynamic behaviour was also revealed in the ^1H NMR spectrum, since at −40°C there were two sets of resonances. Those for the $C(H)C_6H_4Me\text{-}4$ protons of the two diastereoisomers of **IIa** are seen at δ 6.13 and 6.16, to be compared with the single peak observed at δ 6.37 for **IIf**.

The interconversion of the diastereoisomers of **IIa**, so as to allow the PPh_3 and $C_6H_4Me\text{-}4$ groups to be either *transoid* or *cisoid* to one another, is attributed to a low energy pathway involving breaking of the weak $Rh\text{–}C(H)C_6H_4Me\text{-}4$ bond [3]. This process would allow rotation of the $B\text{–}C(H)C_6H_4Me\text{-}4$ linkage, which, when followed by reformation of the $Rh\text{–}C(H)C_6H_4Me\text{-}4$ bond, would transform the PPh_3 and $C_6H_4Me\text{-}4$ groups between *cisoid* and *transoid* configurations. Compound **IIf** has a greater potential for forming diastereoisomers than **IIa** since in addition to the chiral $BC(H)C_6H_4Me\text{-}4$ and rhodium centres, the boron atom of the former group is also chiral. However, for steric reasons it is reasonable to consider that only one diastereoisomer of **IIf** might exist.

Treatment of the complexes **IIa**, **IIc**, and **IIe** with $K[BH(CHMeEt)_3]$, followed by addition of $[NEt_4]Cl$, gave the salts **IIIa**, **IIIb**, and **IIIc**, respectively, demonstrating the electrophilic character of the exopolyhedral carbon atoms of the C(H)R groups in the complexes **II** [3]. Similarly, the reaction between **IIf** and the reagent $K[BH(CHMeEt)_3]$, followed by addition of $[NEt_4]Cl$, afforded the related compound $[NEt_4][Rh(CO)(PPh_3)\{\eta^5\text{-}7,9\text{-}C_2B_9H_{10}(CH_2C_6H_4Me\text{-}4)\text{-}10\}]$ (**IIId**). Data fully characterising this product are given in Tables 1–3, and are similar to those of its isomer **IIIa**, after allowing for variations arising because of the different 2,1,7- and 3,1,2-RhC_2B_9 icosahedral core structures of the two species. The $^{31}P\text{-}\{^1H\}$ NMR spectrum of **IIId** shows a doublet resonance at δ 35.7 [*J*(RhP) 164 Hz] to be compared with the corresponding doublet in the spectrum of **IIIa** at δ 33.7 [*J*(RhP) 154 Hz] [3]. The linkage of the $CH_2C_6H_4Me\text{-}4$ group to a chiral boron atom in **IIId** results in non-equivalence of the methylene protons in the ^1H NMR spectrum, due to their being diastereotopic. Thus an AB quartet, integrating for two protons, is observed at δ

TABLE 4. Selected internuclear distances (Å) and angles (°) in the complex $[Rh(CO)(PPh_3)\{\eta^5\text{-}7,9\text{-}C_2B_9H_{10}[C(H)(C_6H_4Me\text{-}4)(PEt_3)]\text{-}10\}]\cdot CH_2Cl_2$ (**IVb**)

Rh–P(1)	2.286(2)	Rh–B(1)	2.275(6)	Rh–C(2)	2.331(5)	Rh–B(3)	2.261(7)
Rh–C(4)	2.357(6)	Rh–B(5)	2.210(7)	Rh–C(5)	1.804(6)	P(2)–C(10)	1.818(6)
B(1)–C(2)	1.688(8)	B(1)–B(5)	1.863(9)	B(1)–B(6)	1.801(9)	B(1)–B(10)	1.784(9)
B(1)–C(10)	1.650(7)	C(2)–B(3)	1.721(8)	C(2)–B(6)	1.711(9)	C(2)–B(7)	1.686(8)
B(3)–C(4)	1.668(10)	B(3)–B(7)	1.810(10)	B(3)–B(8)	1.808(10)	C(4)–B(5)	1.700(9)
C(4)–B(8)	1.677(10)	C(4)–B(9)	1.679(10)	B(5)–B(9)	1.801(10)	B(5)–B(10)	1.811(10)
B(6)–B(7)	1.765(9)	B(6)–B(10)	1.741(10)	B(6)–B(11)	1.741(9)	B(7)–B(8)	1.776(11)
B(7)–B(11)	1.790(11)	B(8)–B(9)	1.767(11)	B(8)–B(11)	1.785(11)	B(9)–B(10)	1.769(9)
B(9)–B(11)	1.763(11)	B(10)–B(11)	1.790(10)	C(5)–O(5)	1.145(9)	C(10)–C(11)	1.527(7)
P(1)–Rh–B(1)	144.1(2)	P(1)–Rh–C(2)	109.0(1)	B(1)–Rh–C(2)	43.0(2)		
P(1)–Rh–B(3)	95.6(2)	B(1)–Rh–B(3)	77.0(2)	C(2)–Rh–B(3)	44.0(2)		
P(1)–Rh–C(4)	121.3(2)	B(1)–Rh–C(4)	76.2(2)	C(2)–Rh–C(4)	71.0(2)		
B(3)–Rh–C(4)	42.3(2)	P(1)–Rh–B(5)	163.2(2)	B(1)–Rh–B(5)	49.1(2)		
C(2)–Rh–B(5)	75.4(2)	B(3)–Rh–B(5)	76.1(3)	C(4)–Rh–B(5)	43.6(2)		
P(1)–Rh–C(5)	89.9(2)	B(1)–Rh–C(5)	105.0(3)	C(2)–Rh–C(5)	143.9(3)		
B(3)–Rh–C(5)	167.0(3)	C(4)–Rh–C(5)	125.2(3)	B(5)–Rh–C(5)	95.4(3)		
Rh–B(1)–C(2)	70.3(3)	Rh–B(1)–B(5)	63.7(3)	C(2)–B(1)–B(5)	102.8(4)		
Rh–B(1)–C(10)	106.4(4)	C(2)–B(1)–C(10)	122.0(4)	B(5)–B(1)–C(10)	128.4(5)		
B(10)–B(1)–C(10)	124.3(5)	Rh–C(2)–B(1)	66.7(3)	Rh–C(2)–B(3)	65.9(3)		
B(1)–C(2)–B(3)	111.9(4)	Rh–B(3)–C(2)	70.1(3)	Rh–B(3)–C(4)	71.9(3)		
C(2)–B(3)–C(4)	106.9(5)	Rh–C(4)–B(3)	65.8(3)	Rh–C(4)–B(5)	63.6(3)		
B(3)–C(4)–B(5)	109.8(4)	Rh–B(5)–B(1)	67.3(3)	Rh–B(5)–C(4)	72.8(3)		
B(1)–B(5)–C(4)	106.6(4)	B(8)–B(9)–B(10)	108.5(5)	B(6)–B(10)–B(9)	107.6(5)		
B(7)–B(8)–B(9)	107.2(5)	B(6)–B(7)–B(8)	107.6(5)	B(7)–B(6)–B(10)	108.9(5)		
Rh–C(5)–O(5)	176.8(6)	P(2)–C(10)–B(1)	119.9(4)	P(2)–C(10)–C(11)	109.6(4)		
B(1)–C(10)–C(11)	114.5(4)						

2.45 and 2.54 [J(AB) 12 Hz] (Table 2). This contrasts with the ^{1}H NMR spectrum of **IIIa** where only a broad signal is seen at δ 2.48 [3], because the CH_2 protons are equivalent since the boron atom CCB*B*B to which the $CH_2C_6H_4$Me-4 fragment is attached is not chiral. In the ^{13}C-{^{1}H} NMR spectrum of **IIId** resonances for the cage CH vertices occur at δ 45.6 and 41.7, with the signal for the B*C*H_2 nucleus appearing as a very broad peak at δ 33.7, the broadness presumably due to unresolved ^{11}B–^{13}C coupling. In the ^{13}C-{^{1}H} NMR spectrum of **IIIa** the resonance for the B*C*H_2 nucleus is at δ 34.2 [3].

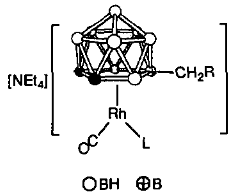

	R	L	●
IIIa	C_6H_4Me-4	PPh_3	CH
IIIb	$C_6H_3Me_2$-2,6	PPh_3	CH
IIIc	C_6H_4Me-4	CO	CMe

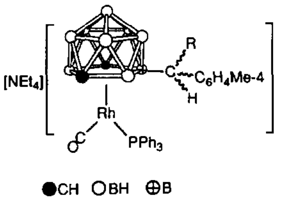

	R
IIId	H
IIIe	Me

Having established that the exopolyhedral carbon atom in **IIf** was susceptible to nucleophilic attack by H^-, it was decided to investigate whether the carbon atom would add tertiary phosphines to form ylide type structures. Treatment of **IIf** in THF with PMe_3, PEt_3, or PMe_2Ph gave, respectively, the zwitterionic complexes [Rh(CO)(PPh_3){η^5-7,9-$C_2B_9H_{10}$[C(H)(R)(L)]-10}] (R = C_6H_4Me-4, L = PMe_3 (**IVa**), PEt_3 (**IVb**), or PMe_2Ph (**IVc**)), characterised by the data given in Tables 1–3. Duplication of some resonances in the NMR spectra of these products revealed that they were each formed as a mixture of two diastereoisomers, one of which was present in solution in very minor amount, typically 10% or less based on peak intensities. Discussion of the NMR data is deferred, however, until the results of an X-ray diffraction study on **IVb** are described.

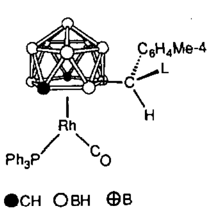

	L
IVa	PMe_3
IVb	PEt_3
IVc	PMe_2Ph

Selected bond distances and angles are given in Table 4, and the molecule **IVb** is shown in Fig. 1. The exopolyhedral carbon atom C(10) is chiral, so that in one of the two diastereoisomers the H, PEt_3, and C_6H_4Me-4 groups will be arranged in this clockwise order when viewed along the C(10)–B bond towards the boron atom in the CBCBB face of the cage, while the other diastereoisomer will have an H, C_6H_4Me-4, PEt_3 orientation. It is seen from Fig. 1 that the former configuration is the one revealed by the X-ray diffraction study. Moreover, NMR measurements on solutions of the crystals employed in the X-ray work revealed that they were those of the major isomer. The molecular structure also clearly shows that the PPh_3, PEt_3 and C_6H_4Me-4 groups are oriented so that they point away from each other, an arrangement one would anticipate based on steric considerations. Significantly also, the PPh_3 ligand is orientated such that it is as far away from C(10) as possible. One may postulate that as the PEt_3 molecule attacks the exopolyhedral C atom in **IIf**, rupture of the Rh–C σ bond is accompanied by rotation of the Rh(CO)(PPh_3) unit, so as to move the bulky PPh_3 ligand away from the sterically demanding C(H)(C_6H_4Me-4)(PEt_3) fragment. Furthermore, the orientation of the Rh(CO)(PPh_3) moiety in the precursor **IIf**, assuming it has a *transoid* P–Rh–C structure similar to that established for **IIa** [3], would clearly make it very unlikely for the PEt_3 molecule to attack the carbon atom in the former species from below the plane of the C(H)C_6H_4Me-4 fragment. This accounts for the predominance of the diastereoisomer identified in the X-ray diffraction study which is the isomer which would result from approach of the PEt_3 molecule from above and to the right of the μ-C(H)C_6H_4Me-4 group in **IIf**, as depicted in the structural formula of **IVb**.

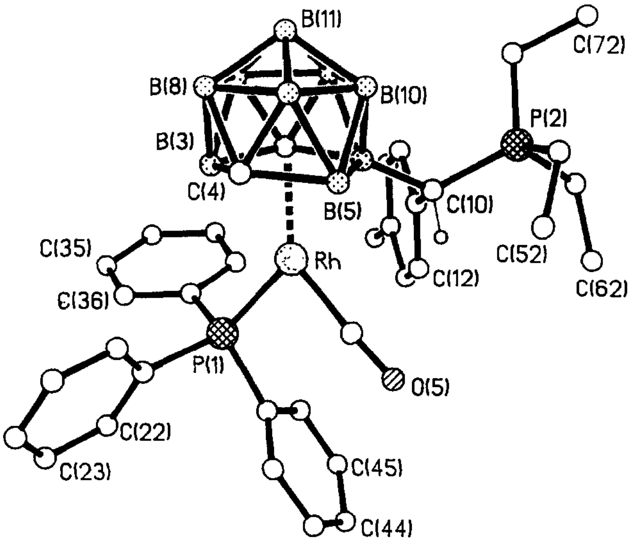

Fig. 1. The molecular structure of [Rh(CO)(PPh_3)(η^5-7,9-$C_2B_9H_{10}$-[C(H)(C_6H_4Me-4)(PEt_3)]-10}] (**IVb**), showing the crystallographic numbering scheme.

The crystal structure of **IVb** having been established, the NMR data (Tables 2 and 3) are readily interpreted. In the ^{31}P-{^{1}H} NMR spectrum the resonance for the

PPh_3 ligand occurs as a very broad doublet at δ 36.4 [J(RhP) 164 Hz]. No signal for the PPh_3 group of the minor isomer was detected due either to the weakness or broadness of the resonance, or because it was hidden by the broad doublet of the major isomer. The resonance for the PEt_3 group of the major isomer occurs at δ 38.5, and for the minor isomer at δ 38.4. The relative intensity of these peaks was *ca.* 18 : 1, and as expected there was no ^{103}Rh–^{31}P coupling on either signal, both signals being sharp singlets. The chemical shifts for the PEt_3 groups in the two isomers are similar to that observed (δ 35.5) in the spectrum of the zwitterionic complex $[Cr(CO)_3\{\eta^5\text{-}C_5H_4(CH_2PEt_3)\}]$ [5]. In the $^{11}B\text{-}\{^1H\}$ NMR spectrum of **IVb** the resonances for the $\mathit{B}C(H)(C_6H_4Me\text{-}4)(PEt_3)$ nuclei of the major and minor isomers occur at δ −5.0 and −6.8, respectively. These shifts are appreciably more shielded than those customarily observed for cage boron atoms bonded to exopolyhedral carbons which generally occur in the range δ *ca.* 1 to 12 [6]. However, the $C(H)(C_6H_4Me\text{-}4)(L)$ groups in the compounds **IV**, with their tertiary phosphine substituents, are without precedent, and there is no doubt about the assignment of the peaks at δ −5.0 and −6.8 because in a fully coupled ^{11}B NMR spectrum of **IVb** they remain as singlets whereas all the resonances for the BH groups (δ −13.1 to −26.6) become doublets.

In the $^{13}C\text{-}\{^1H\}$ NMR spectrum of **IVb** only the resonance for the $B\mathit{C}(H)(C_6H_4Me\text{-}4)(PEt_3)$ nucleus of the major isomer is seen (δ 33.9). Six peaks are observed for the carbon nuclei of the C_6H_4 ring, a feature diagnostic for hindered rotation about the C(10)–C(11) bond (Fig. 1) [7]. The large PEt_3 group evidently prevents free rotation. The cage CH vertices of **IVb** are clearly inequivalent with two resonances being seen at δ 45.6 and 44.7. Signals for the cage CH and CO groups of the minor diastereoisomer are not observed, but the resonance for the CO ligand of the major isomer occurs as a doublet of doublets of doublets at δ 197.0 [J(RhC) 92, J(PC) 22 and 4 Hz]. The ^{1}H NMR spectrum is as expected, allowing for the fact that few peaks for the minor isomer are revealed due to its low concentration. A diagnostic resonance [6] for the $BC(\mathit{H})(C_6H_4Me\text{-}4)(PEt_3)$ proton occurs at δ 4.32 as a broad doublet [J(PH) 21 Hz]. The CH_2 protons of the PEt_3 moiety give rise to a complex pattern (Table 2) as a consequence of their being diastereotopic. The spectroscopic data for **IVa** and **IVc** may be interpreted in a similar manner to those of **IVb**, leaving no doubt that all three compounds have similar structures. Although the $^{13}C\text{-}\{^1H\}$ NMR spectra of **IVa** and **IVc** were insufficiently resolved in the aromatic region to allow all resonances to be identified, it was evident that for these species also the C_6H_4 fragment displays more than four signals, in accord with restricted rotation about the $C\text{–}C^1(C_6H_4Me\text{-}4)$ bond.

The reaction between compound **IIf** and MeLi was also investigated and found to give a chromatographically inseparable mixture (*ca.* 2:3) of $[NEt_4][Rh(CO)(PPh_3)\{\eta^5\text{-}7,9\text{-}C_2B_9H_{10}[C(H)(Me)(C_6H_4Me\text{-}4)]\text{-}10\}]$ (**IIIe**) and $[NEt_4][Rh(COMe)\{\sigma,\eta^5\text{-}7,9\text{-}C_2B_9H_{10}[C(H)C_6H_4Me\text{-}4]\text{-}10\}(PPh_3)]$ (**V**). The NMR signals recorded on mixtures of these two products were well resolved, allowing the resonances for both to be assigned on the basis of the observed chemical shifts, coupling constants, and peak intensities. Moreover, the NMR data revealed that both **IIIe** and **V** exist as single diastereoisomers. Since the two complexes are isomers, microanalysis of the mixture (Table 1) was indicative of the composition.

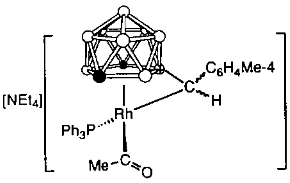

V

●CH ○BH ⊕B

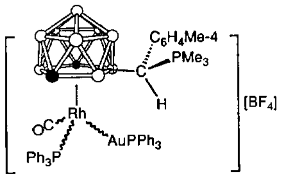

VI

Clearly **IIIe** arises from nucleophilic attack of Me^- on the exopolyhedral bridging carbon atom of **IIf**, whereas **V** results from attack on the carbonyl ligand. Since the two compounds are so disparate, and there is no interconversion between them, it is reasonable for their spectroscopic properties to be discussed separately. In the $^{11}B\text{-}\{^1H\}$ NMR spectrum of **IIIe** there is a diagnostic resonance for the $\mathit{B}C(H)(Me)(C_6H_4Me\text{-}4)$ nucleus at δ 3.0, and correspondingly in the $^{13}C\text{-}\{^1H\}$ NMR spectrum there is a very broad peak for the $B\mathit{C}(H)(Me)(C_6H_4Me\text{-}4)$ carbon atom at δ 33.7. In the latter spectrum the CO resonance occurs as a doublet of doublets at δ 198.2 [J(RhC) 92, J(PC) 21 Hz]. This observation clarifies the somewhat unexpected pattern seen for the CO resonance in the spectrum of **IVb** which, as mentioned above, occurs as a doublet of doublets of doublets (J 92, 22, and 4 Hz). Clearly the small 4 Hz coupling must be a ^4J(PC) coupling with the PEt_3 group. Interestingly, the C_6H_4 group in the $^{13}C\text{-}\{^1H\}$ NMR spectrum of **IIIe** gives rise to the customary four peaks, indicating free rotation about the $C\text{–}C^1(C_6H_4Me\text{-}4)$ bond. This is in contrast with the six signals for the C_6H_4 group seen in the spectrum of **IVb**, mentioned earlier. Since the Me group in **IIIb** is appreciably less sterically demanding than the tertiary phosphine molecules present in the complexes **IV** it is not surprising that rotation about the $C\text{–}C^1(C_6H_4Me\text{-}4)$ bond can take place in **IIIe**.

Owing to the presence of the peaks from the NEt_4^+ counter ion in **IIIe**, in the ^{1}H NMR spectrum it was initially impossible to detect the resonances due to the BC(*H*)(*Me*)(C_6H_4*Me*-4) protons. Accordingly the synthesis was repeated using $[N(PPh_3)_2]^+$ as the counter ion. This allowed the signal for the BC(H)*Me* group to be measured as a doublet [*J*(HH) 7 Hz] at δ 1.25, and the BC(*H*)Me proton to be seen as a quartet [*J*(HH) 7 Hz] at δ 3.06. The C_6H_4*Me*-4 protons resonated as a singlet at δ 2.00.

The IR spectrum of **V** displays a broad band at 1600 cm^{-1}, typical for an acyl group. In the ^{13}C-{^1H} NMR spectrum the signal for this group is seen at δ 243.3 [*J*(RhC) 32, *J*(PC) 13 Hz]. A very broad resonance at δ 57.6 must be assigned to the *C*(H)C_6H_4Me-4 nucleus, although it is considerably less deshielded than those observed in the neutral complex **IIf** (δ 80.4) and the other species of type **II** [2e, 3]. In the ^{11}B-{^1H} NMR spectrum the presence of the *B*C(H)C_6H_4Me-4 nucleus is revealed by a resonance at δ 3.0, the remaining boron atoms giving broad overlapping signals in the range δ −11.6 to −28.4.

For all the complexes **III** and **IV** the CO stretches in the IR spectra (Table 1) are at very similar or even the same frequencies as those of the salts **I** (for **Ie**, ν_{max}(CO) is at 1915 cm^{-1} [8]). In contrast, ν_{max}(CO) for **IIf** (2022 cm^{-1}) is *ca.* 100 cm^{-1} higher in frequency. This suggests that in the species **III** and **IV** negative charge resides to an appreciable degree at the metal centres, leading to the expectation that the rhodium atoms in the latter might show nucleophilic character, reacting with electrophiles in certain circumstances, as does rhodium in the reagents **I**. To test this idea the reaction between **IVa** and $[Au(PPh_3)]^+$ was investigated.

Treatment of **IVa** in THF with [AuCl(PPh_3)], in the presence of $TlBF_4$, afforded the green complex [RhAu(CO)(PPh_3)$_2${η^5-7,9-$C_2B_9H_{10}$[C(H)(C_6H_4Me-4)(PMe$_3$)]-10}][BF_4] (**VI**), fully characterised by the data given in Tables 1–3. The salt **VI** is closely related to the neutral complexes [RhAu(CO)(PPh_3)$_2$(η^5-7,*n*-$C_2B_9H_{11}$)] (*n* = 8 [2b] or 9 [2g]) obtained by treating the salts **Ib** or **Ie**, respectively, with [AuCl(PPh_3)] in the presence of $TlBF_4$ to facilitate removal of chloride as insoluble TlCl.

The ^{31}P-{^1H} NMR spectrum of **VI** has resonances for the Rh(PPh_3) group at δ 34.1 [*J*(RhP) 126 Hz], the PMe_3 group at δ 33.7, and the Au(PPh)$_3$ group at δ 30.7 [*J*(RhP) 4 Hz]. No other signals were observed, indicating that only one diastereoisomer was formed, probably for steric reasons connected with the bulky Au(PPh)$_3$ group. In the ^{31}P-{^1H} NMR spectrum of [RhAu(CO)(PPh_3)$_2$(η^5-7,9-$C_2B_9H_{11}$)] resonances for the Rh(PPh_3) and Au(PPh_3) groups are seen at δ 36.4 [*J*(RhP) 132 Hz] and 33.2, respectively [2g]. In the IR spectrum of this compound the CO stretch is at 1993 cm^{-1}, to be compared with that at 1972 cm^{-1} for **VI**. The latter value reflects the different Rh–CO bonding in the two complexes. The CO absorption for **VI** is appreciably lower than one would expect for a cationic carbonyl complex, and must be a consequence of the positive charge being some distance away at the phosphorus atom, thus allowing significant back bonding from the rhodium to the carbonyl ligand. The shift in frequency from 1927 cm^{-1} in **IVa** to 1972 cm^{-1} in **VI** is, however, consistent with a transition from an anionic- to a cationic- type rhodium complex, lending credence to the proposal that there is significant separation and localisation of the positive and negative charges in the zwitterionic compounds **IV**. Thus effectively, in the formation of **VI** from **IVa** the rhodium centre has gone from being anionic in character to neutral. In accord with this, the magnitude of the ^{103}Rh–^{13}CO coupling in the ^{13}C-{^1H} NMR spectrum decreases from 92 Hz in **IVa** to 76 Hz in **VI**, a value very close to that (73 Hz) in [RhAu(CO)(PPh_3)$_2$(η^5-7,9-$C_2B_9H_{11}$)] [2g]. The 92 Hz ^{103}Rh–^{13}CO coupling for **IVa** is typical for a rhodium complex in which the metal centre carries a negative charge.

The ^{13}C-{^1H} NMR spectrum of **VI** shows resonances for the non-equivalent cage CH vertices at δ 57.9 and 51.4, a very broad peak for the B*C*(H)(C_6H_4Me-4)(PMe_3) atom at δ 37.2, and peaks for the Me-4 and PMe_3 groups at δ 21.3 and 10.6 [*J*(PC) 54 Hz], respectively. In the ^1H NMR spectrum the BC(*H*)(C_6H_4Me-4)(PMe_3) is a doublet at δ 3.67 [*J*(PH) 22 Hz], and in the ^{11}B-{^1H} NMR spectrum the signal at δ 0.4 is assigned to the *B*C(H)(C_6H_4Me-4)(PMe_3) nucleus. In agreement this resonance remains a singlet in a proton-coupled ^{11}B spectrum.

The reactions reported in this paper illustrate the reactive nature of the μ-C(H)R groups in the complexes **II** and the nucleophilicity of the rhodium centres in the compounds **IV**. Both observations exemplify the potential of these compounds for further syntheses.

3. Experimental section

Light petroleum refers to the fraction of b.p. 40–60°C. All solvents were distilled over appropriate drying agents prior to use. Chromatography columns, *ca.* 15 cm long and 3 cm wide, were packed with alumina (Brockmann activity II). Celite pads used to remove TlCl by filtration, were *ca.* 3 cm thick. All experiments were carried out under nitrogen by using Schlenk-tube techniques. The NMR measurements were made with a Bruker AMX 360 MHz instrument. Throughout this paper chemical shifts (δ) are expressed in ppm. The IR spectra were recorded with a Bruker IFS 25 spectrometer. The reagents [NEt_4][Rh(CO)(PPh_3)(η^5-7,9-$C_2B_9H_{11}$)] (**Ie**) [8], [Mn($\equiv$CC_6H_4Me-4)(CO)$_2$(η^5-C_5H_4Me)]

[BCl_4] [9], and [AuCl(PPh_3)] [10] were prepared by procedures previously described. The reagent K[BH(CHMeEt)$_3$] (1.0 mol dm^{-3} solution in THF) was obtained from Aldrich Chemicals. Analytical and other data for the new compounds are given in Table 1.

3.1. Synthesis of [Rh{σ,η^5-7,9-$C_2B_9H_{10}$[C(H)C_6H_4Me-4]-10}(CO)(PPh_3)]

A CH_2Cl_2 (25 cm^3) solution of **Ie** (0.50 g, 0.76 mmol) was saturated with CO gas, [Mn($\equiv$CC_6H_4Me-4)(CO)$_2$(η^5-C_5H_4Me)][BCl_4] (0.34 g, 0.76 mmol) was added, and the mixture stirred under CO for *ca.* 5 min. Solvent was removed *in vacuo* and the residue dissolved in CH_2Cl_2-light petroleum (10 cm^3, 3:2) and chromatographed on alumina at −10°C. Elution with the same solvent mixture afforded an orange eluate. Solvent was removed *in vacuo* and the residue crystallised from CH_2Cl_2-light petroleum (50 cm^3, 1:20) to give the product as an orange oil due to the presence of [Mn(CO)$_3$(η^5-C_5H_4Me)], another product of the reaction. Trituration with light petroleum (50 cm^3) for *ca.* 2 h afforded orange microcrystals of [Rh{σ,η^5-7,9-$C_2B_9H_{10}$[C(H)C_6H_4Me-4]-10}(CO)(PPh_3)] (**IIf**), and removed the [Mn(CO)$_3$(η^5-C_5H_4Me)], which is soluble in light petroleum. The product was washed with light petroleum (2 × 25 cm^3) and dried *in vacuo* (0.40 g).

3.2. Reactions of the complex [Rh{σ,η^5-7,9-$C_2B_9H_{10}$-[C(H)C_6H_4Me-4]-10}(CO)(PPh_3)]

(i) A THF (20 cm^3) solution of **IIf** (0.15 g, 0.24 mmol) was treated with K[BH(CHMeEt)$_3$] (0.27 cm^3, 0.27 mmol) and the mixture stirred for *ca.* 15 min, after which [NEt_4]Cl (0.048 g, 0.27 mmol) was added and the mixture further stirred for 1 h. Solvent was removed *in vacuo* and the yellow-green residue extracted with CH_2Cl_2 (2 × 20 cm^3); the extracts were filtered through a Celite pad to give a green solution, from which the solvent was removed *in vacuo*. The residue was redissolved in the minimum of CH_2Cl_2 (3 cm^3) and Et_2O (50 cm^3) was added dropwise with vigorous stirring to afford a green oil. This oil was washed with Et_2O (2 × 20 cm^3) and then triturated with light petroleum (50 cm^3) for *ca.* 1 h to give dark green microcrystals of [NEt_4][Rh(CO)(PPh_3){η^5-7,9-$C_2B_9H_{10}$($CH_2C_6H_4$Me-4)-10}] (**IIId**), which were washed with light petroleum (2 × 10 cm^3) and dried *in vacuo* (0.18 g).

(ii) To a THF (15 cm^3) solution of **IIf** (0.10 g, 0.16 mmol) was added PMe_3 (0.30 cm^3 of a 0.5 mol dm^{-3} solution in THF, 0.16 mmol). The mixture lightened immediately and was stirred for *ca.* 15 min, after which the solvent was removed *in vacuo*. The orange residue was dissolved in CH_2Cl_2-light petroleum (5 cm^3, 3:2) and chromatographed on alumina at −10°C. Elution with the same solvent mixture afforded initially an orange fraction, followed by a yellow band. The orange band was collected and subsequently shown by IR and NMR spectroscopy to be a trace of unreacted **IIf**. The yellow band was eluted with pure CH_2Cl_2, affording a green-yellow solution. Removal of solvent *in vacuo*, followed by crystallisation from CH_2Cl_2-light petroleum (30 cm^3, 1:10) gave green-yellow microcrystals of [Rh(CO)(PPh_3){η^5-7,9-$C_2B_9H_{10}$[C(H)(C_6H_4Me-4)(PMe_3)]-10}] (**IVa**), which were washed with light petroleum (2 × 10 cm^3) and dried *in vacuo* (0.11 g).

(iii) Similarly a THF (15 cm^3) solution of **IIf** (0.10 g, 0.16 mmol) was treated with PEt_3 (0.024 cm^3, 0.16 mmol), causing the solution to lighten in colour immediately from dark orange to golden yellow. After *ca.* 5 min stirring the solvent was removed *in vacuo*. The resulting residue was dissolved in CH_2Cl_2-light petroleum (5 cm^3, 3:2) and chromatographed on alumina at −10°C. Elution with the same solvent mixture afforded a yellow eluate. Removal of solvent *in vacuo*, followed by crystallisation from CH_2Cl_2-light petroleum (20 cm^3, 1:10) gave yellow microcrystals of [Rh(CO)(PPh_3){η^5-7,9-$C_2B_9H_{10}$[C(H)(C_6H_4Me-4)(PEt_3)]-10}] (**IVb**), which were washed with light petroleum (2 × 10 cm^3) and dried *in vacuo* (0.10 g).

(iv) In a similar experiment, involving stirring of **IIf** in THF (15 cm^3) with PMe_2Ph (0.32 cm^3 of a 0.5 mol dm^{-3} solution in THF, 0.16 mmol) for *ca.* 10 min, chromatographing as above, and crystallising the yellow eluate from CH_2Cl_2-light petroleum (20 cm^3, 1:4), afforded yellow microcrystals of [Rh(CO)(PPh_3){η^5-7,9-$C_2B_9H_{10}$[C(H)(C_6H_4Me-4)(PMe_2Ph)]-10}] (**IVc**), (0.10 g).

(v) Compound **IIf** (0.20 g, 0.32 mmol) in THF (15 cm^3) was treated with MeLi (0.23 cm^3, 0.32 mmol), the mixture immediately darkening to red. After *ca.* 15 min stirring [NEt_4]Cl (0.071 g, 0.39 mmol) was added, and the mixture stirred for a further 30 min. The solvent was then removed *in vacuo*, the resulting red residue extracted with CH_2Cl_2 (2 × 20 cm^3) and the extracts were filtered through a Celite pad to afford a dark red filtrate. Solvent was removed *in vacuo*, and the oily residue crystallised from CH_2Cl_2-light petroleum (20 cm^3, 1:6) to give a red oil, which was washed with light petroleum (2 × 10 cm^3) and then triturated with Et_2O (*ca.* 50 cm^3) for *ca.* 1 h to afford a red powder, which was dried *in vacuo*. IR and NMR spectroscopy established that this was an inseparable mixture of the complexes, [NEt_4][Rh(CO)(PPh_3){η^5-7,9-$C_2B_9H_{10}$[C-(H)(Me)(C_6H_4Me-4)]-10}] (**IIIe**), and [NEt_4][Rh(COMe){σ,η^5-7,9-$C_2B_9H_{10}$[C(H)C_6H_4Me-4]-10}(PPh_3)] (**V**) (0.24 g), formed in *ca.* 2:3 ratio, based on the relative intensities of the ^{31}P and ^{1}H NMR resonances of the mixture.

TABLE 5. Crystal data for compound **IVb**

Molecular formula	$C_{35}H_{48}B_9OP_2Rh \cdot CH_2Cl_2$
M	831.8
Crystal system	Monoclinic
Space group	$P2_1/n$ (non-standard No. 14)
a/Å	13.027(4)
b/Å	17.415(4)
c/Å	18.501(5)
β/°	98.92(2)
U/Å^3	4146(2)
Z	4
D_c/Mg m^{-3}	1.33
$F(000)$	1712
μ(Mo Kα)/cm^{-1}	6.47
T/K	295
Diffractometer	Siemens R3m/V
Scan type	Wyckoff ω
Scan speed/° min.$^{-1}$	2–14.65
Scan range (ω°)	1.20
2θ range (°)	5.0–50.0
Radiation	Mo Kα ($\bar{\lambda}$, 0.71073 Å)
Collected data	7917
Unique data	7298
Observed data [$F \geq 5.0\sigma(F)$]	5133
Data-to-parameter ratio	10.3:1
Weighting scheme	$w^{-1} = [\sigma^2(F) + 0.0005\,\lvert F \rvert^2]$
R, R_w	0.049, 0.048
Residual density (max., min./eÅ^{-3})	1.03, −1.01

3.3. *Reaction of* $[AuCl(PPh_3)]$ *with* $[Rh(CO)(PPh_3)\{\eta^5\text{-}7,9\text{-}C_2B_9H_{10}[C(H)(C_6H_4Me\text{-}4)(PMe_3)]\text{-}10\}]$

The compounds **IVa** (0.080 g, 0.11 mmol), $[AuCl(PPh_3)]$ (0.056 g, 0.11 mmol), and $TlBF_4$ (0.036 g, 0.12 mmol) were stirred in THF (20 cm^3) for *ca.* 2 h. The mixture was then filtered through a Celite pad, to remove TlCl, giving a pale yellow-green solution. Solvent was removed *in vacuo*, and the residue crystallised from CH_2Cl_2-light petroleum (20 cm^3, 1:6) to afford pale green microcrystals of $[RhAu(CO)(PPh_3)_2\{\eta^5\text{-}7,9\text{-}C_2B_9H_{10}[C(H)(C_6H_4Me\text{-}4)(PMe_3)]\text{-}10\}][BF_4]$ (**VI**), which were washed with light petroleum (2 × 5 cm^3) and dried *in vacuo* (0.13 g).

3.4. *Crystal structure determination*

Crystals of compound **IVb** were grown from a CH_2Cl_2-light petroleum (6 cm^3, 1:5) solution. The X-ray data were obtained from a clear yellow rectangular crystal (0.41 × 0.42 × 0.61 mm). Crystal data and relevant parameters are summarised in Table 5. The collected intensities showed no signs of significant decay. After the intensity data were corrected for Lorentz and polarization effects, an empirical absorption correction was applied.

The structure was solved by Patterson and Fourier methods using the SHELXTL package [11]. The structure was refined by full-matrix least-squares, with anisotropic thermal parameters for all non-hydrogen atoms. The hydrogen atoms attached to the boron atoms and C(10) were located and refined with fixed isotropic thermal parameters (U_{iso} = 0.08 Å^2). All remaining hydrogen

TABLE 6. Atomic positional parameters (fractional coordinates × 10^4) for **IVb**, with estimated standard deviations in parentheses

	x	y	z
Rh	2201(1)	1994(1)	1409(1)
P(1)	1468(1)	3003(1)	1934(1)
P(2)	2011(1)	925(1)	−1029(1)
B(1)	2910(5)	1623(4)	416(3)
C(2)	3441(4)	2463(3)	739(3)
B(3)	3852(5)	2430(4)	1669(3)
C(4)	3845(5)	1509(4)	1916(3)
B(5)	3157(5)	983(4)	1232(4)
B(6)	4177(5)	1917(4)	247(3)
B(7)	4739(5)	2467(5)	1007(4)
B(8)	5005(6)	1838(5)	1768(4)
B(9)	4549(6)	918(4)	1468(4)
B(10)	3992(5)	982(4)	535(4)
B(11)	5150(5)	1503(5)	878(4)
C(5)	993(5)	1473(4)	1340(4)
O(5)	251(4)	1111(3)	1292(4)
C(10)	1947(4)	1586(3)	−277(3)
C(11)	1568(4)	2369(3)	−579(3)
C(12)	579(4)	2632(3)	−506(3)
C(13)	224(4)	3340(3)	−776(3)
C(14)	831(4)	3813(3)	−1128(3)
C(15)	1817(5)	3562(3)	−1207(3)
C(16)	2169(4)	2846(3)	−936(3)
C(17)	450(5)	4593(3)	−1410(4)
C(21)	1686(4)	3066(3)	2938(3)
C(22)	1131(4)	3580(3)	3312(3)
C(23)	1273(5)	3598(3)	4065(3)
C(24)	1995(5)	3110(4)	4456(3)
C(25)	2565(5)	2606(4)	4096(3)
C(26)	2401(5)	2589(3)	3338(3)
C(31)	1864(4)	3949(3)	1635(3)
C(32)	1840(4)	4066(3)	885(3)
C(33)	2157(5)	4762(4)	633(3)
C(34)	2519(5)	5337(3)	1104(4)
C(35)	2568(5)	5222(3)	1847(4)
C(36)	2246(4)	4535(3)	2108(3)
C(41)	42(4)	3021(3)	1749(3)
C(42)	−508(5)	2564(4)	2172(4)
C(43)	−1577(5)	2476(5)	2007(5)
C(44)	−2116(5)	2859(5)	1405(5)
C(45)	−1594(5)	3310(5)	988(4)
C(46)	−510(4)	3393(4)	1144(3)
C(51)	2017(5)	−49(4)	−716(4)
C(52)	1410(7)	−224(5)	−125(5)
C(61)	877(5)	1097(5)	−1739(4)
C(62)	−155(6)	942(5)	−1519(5)
C(71)	3123(5)	1054(4)	−1484(3)
C(72)	3156(6)	552(5)	−2154(4)
Cl(1)	6156(4)	4748(3)	977(3)
Cl(2)	5424(5)	5704(5)	1867(4)
Cl(3)	5118(6)	6203(6)	887(8)
C	5102(16)	5204(13)	1187(12)

atoms were included in calculated positions (C–H = 0.96 Å) with fixed isotropic thermal parameters (U_{iso} = 0.08 $Å^2$). The asymmetric unit contains a badly disordered molecule of CH_2Cl_2. One of the Cl atoms [Cl(1)] has a reasonably well defined location but it was necessary to refine the second Cl atom as two separate components [Cl(2) and Cl(3)] each having a 50% site occupancy. The final difference Fourier map showed the highest peak to be 1.03 e $Å^{-3}$, this being in the vicinity of the disordered solvent molecule. Atomic scattering factors were taken from ref. [12]. Final atomic positional parameters for non-hydrogen atoms are given in Table 6.

Additional data available from the Cambridge Crystallographic Data Centre comprises H-atom coordinates, anisotropic thermal parameters, and remaining bond lengths and angles.

Acknowledgments

We thank the UK Science and Engineering Research Council for a research studentship for J.E.G., and the Robert A. Welch Foundation for a Grant (AA-1201) in support of the preparative work, which was carried out at Baylor University.

References and notes

1 In the complexes discussed in this paper rhodium atoms form with $[nido\text{-}7,n\text{-}C_2B_9H_9R'_2]^{2-}$ (n = 8 or 9) anions *closo*-1,2-dicarba-3-rhodadodecaborane and *closo*-1,7-dicarba-2-rhodadodecaborane structures, respectively. In the formulae the carborane groups are designated as $\eta^5\text{-}C_2B_9H_9R'_2$ in order to emphasise their pentahapto ligand properties in which these *nido*-fragments formally act as four electron donors. We therefore treat the cages in the products as *nido*-11-vertex ligands with the numbering as for an icosahedron from which the twelfth vertex has been removed, in order to avoid a cumbersome labelling system.

2 (a) J.R. Fernandez, G.F. Helm, J.A.K. Howard, M.U. Pilotti and F.G.A. Stone, *J. Chem. Soc., Dalton Trans.*, (1990) 1747; (b) N. Carr, M.C. Gimeno, J.E. Goldberg, M.U. Pilotti, F.G.A. Stone and I. Topaloğlu, *J. Chem. Soc., Dalton Trans.*, (1990) 2253; (c) J.E. Goldberg, J.A.K. Howard, H. Müller, M.U. Pilotti and F.G.A. Stone, *J. Chem. Soc., Dalton Trans.*, (1990) 3055; (d) M.U. Pilotti, I. Topaloğlu and F.G.A. Stone, *J. Chem. Soc., Dalton Trans.*, (1991) 1355; (e) M.U. Pilotti, F.G.A. Stone and I. Topaloğlu, *J. Chem. Soc., Dalton Trans.*, (1991) 1621; (f) J.E. Goldberg, D.F. Mullica, E.L. Sappenfield and F.G.A. Stone, *J. Chem. Soc., Dalton Trans.*, (1992) 2693; (g) J.E. Goldberg and F.G.A. Stone, *Polyhedron, 11* (1992) 2841; (h) J.C. Jeffery, F.G.A. Stone and I. Topaloğlu, *J. Organomet. Chem.*, in press.

3 M.U. Pilotti and F.G.A. Stone, *J. Chem. Soc., Dalton Trans.*, (1990) 2625.

4 D.D. Devore, C. Emmerich, J.A.K. Howard and F.G.A. Stone, *J. Chem. Soc., Dalton Trans.*, (1989) 797.

5 O. Koch, F. Edelmann and U. Behrens, *Chem. Ber., 115* (1982) 1313.

6 S.A. Brew and F.G.A. Stone, *Adv. Organomet. Chem., 35* (1993) 135.

7 D.G. Evans, J.A.K. Howard, J.C. Jeffery, D.B. Lewis, G.E. Lewis, M.J. Grosse-Ophoff, M.J. Parrott and F.G.A. Stone, *J. Chem. Soc., Dalton Trans.*, (1986) 1723; N. Carr, J.R. Fernandez and F.G.A. Stone, *Organometallics, 10* (1991) 2718.

8 J.A. Walker, C.B. Knobler and M.F. Hawthorne, *Inorg. Chem., 24* (1985) 2688.

9 E.O. Fischer, E.W. Meineke and F.R. Kreissl, *Chem. Ber., 110* (1977) 1140; E.O. Fischer and G. Besl, *Z. Naturforsch., B34* (1979) 1186; E.O. Fischer, J.K.R. Wanner, G. Müller and J. Reide, *Chem. Ber., 118* (1985) 3311.

10 R. Usón and A. Laguna, *Organomet. Synth., 3* (1986) 325.

11 SHELXTL-PC, Siemens Analytical X-Ray Instruments.

12 *International Tables for X-ray Crystallography*, Kynoch Press, Birmingham, 1974, vol. 4.